JACS
JOURNAL OF THE AMERICAN CHEMICAL SOCIETY

Communication

pubs.acs.org/JACS

Synthesis of Composition Tunable and Highly Luminescent Cesium Lead Halide Nanowires through Anion-Exchange Reactions

Dandan Zhang,[†,§,⊥] Yiming Yang,[†,§,⊥] Yehonadav Bekenstein,[†,§,∥,⊥] Yi Yu,[†,§] Natalie A. Gibson,[†,#] Andrew B. Wong,[†,§] Samuel W. Eaton,[†] Nikolay Kornienko,[†] Qiao Kong,[†] Minliang Lai,[†] A. Paul Alivisatos,[†,‡,§,∥] Stephen R. Leone,[†,#,▽] and Peidong Yang*[,†,‡,§,∥]

[†]Department of Chemistry, [‡]Department of Materials Science and Engineering, and [▽]Department of Physics, University of California, Berkeley, California 94720, United States

[§]Materials Sciences Division and [#]Chemical Sciences Division, Lawrence Berkeley National Laboratory, Berkeley, California 94720, United States

[∥]Kavli Energy NanoSciences Institute, Berkeley, California 94720, United States

Supporting Information

ABSTRACT: Here, we demonstrate the successful synthesis of brightly emitting colloidal cesium lead halide ($CsPbX_3$, X = Cl, Br, I) nanowires (NWs) with uniform diameters and tunable compositions. By using highly monodisperse $CsPbBr_3$ NWs as templates, the NW composition can be independently controlled through anion-exchange reactions. $CsPbX_3$ alloy NWs with a wide range of alloy compositions can be achieved with well-preserved morphology and crystal structure. The NWs are highly luminescent with photoluminescence quantum yields (PLQY) ranging from 20% to 80%. The bright photoluminescence can be tuned over nearly the entire visible spectrum. The high PLQYs together with charge transport measurements exemplify the efficient alloying of the anionic sublattice in a one-dimensional $CsPbX_3$ system. The wires increased functionality in the form of fast photoresponse rates and the low defect density suggest $CsPbX_3$ NWs as prospective materials for optoelectronic applications.

One-dimensional (1D) nanowires (NWs) have been extensively studied for their interesting physical properties and their potential as building blocks for various applications in electronics,[1] optoelectronics,[2] sensing,[3] and energy harvesting[4] at the nanoscale. Current strategies for producing high aspect ratio NWs are mainly based on the vapor−liquid−solid method,[5] the solution−liquid−solid method,[6] template-assisted synthesis,[7] nanoparticle assembly,[8] or surfactant-mediated growth.[9] Although impressive progress has been made in synthesizing high-quality materials with well-defined morphology and composition, the tailored synthesis of NWs with well-controlled size, composition, and properties remains challenging in many cases. The synthesis of high-quality $CsPbX_3$ (X = Cl, Br, I) NWs is one example. We recently reported a catalyst-free, solution-phase synthesis of $CsPbX_3$ NWs,[10] in which $CsPbBr_3$ NWs of uniform diameter and desirable optical properties can be accessed. However, for the other two related compositions (X = Cl, I), the NWs produced via direct synthesis suffered from low NW yield, poor diameter control, or undesirable optical properties. The growing interests in utilizing perovskite nanomaterials for various applications[11] motivated us to pursue alternative methods that can achieve simultaneous synthetic control over both material composition and NW morphology.

Postsynthetic chemical transformations, such as ion-exchange reactions, have proven to be simple and versatile approaches to achieve fine control over material compositions and to create new materials and nanostructures not readily accessible by other techniques.[12] At the nanoscale, ion-exchange reactions have been studied mostly on II−VI, III−V, and IV−VI semiconductor compounds, involving partial or complete replacement of ions of a parent nanostructure by new guest ions. Recently, ion exchange in halide perovskites has rapidly emerged as an effective way to attain broad compositional tunability.[12d−h] Due to the high halide ion mobility[13] and the rigid nature of the cationic sublattice[13b] of halide perovskites, fast and facile anion-exchange reactions have been demonstrated in $CsPbX_3$ quantum dots and have afforded wide compositional and optical tunability.[12e,f]

We thus study the effects of anion-exchange reaction in a 1D halide perovskite system. The $CsPbX_3$ NWs are special members of the colloidal nanostructured perovskite family. While their diameter is only about 10 nm and they are moderately quantum confined, they can be a few microns long, which enables macroscopic exploration of their physical properties. In addition X-ray powder diffraction (XRD) patterns show that the NWs present the signature of the orthorhombic phase, which is lacking in the other members of colloidal synthesized nanostructures, typically being in the metastable cubic phase.[12f,g,14]

Here, anion-exchange reactions were developed and applied to $CsPbBr_3$ NWs by reacting them with other halide precursors. The reactions afford alloy NWs with a wide range of compositions while also preserving the original morphology and crystal structure. The alloy NWs have tunable photoluminescence (PL) spanning over nearly the entire visible spectral region (409−680 nm). Photoluminescence quantum

Received: March 25, 2016
Published: May 23, 2016

© 2016 American Chemical Society

DOI: 10.1021/jacs.6b03134
J. Am. Chem. Soc. 2016, 138, 7236−7239

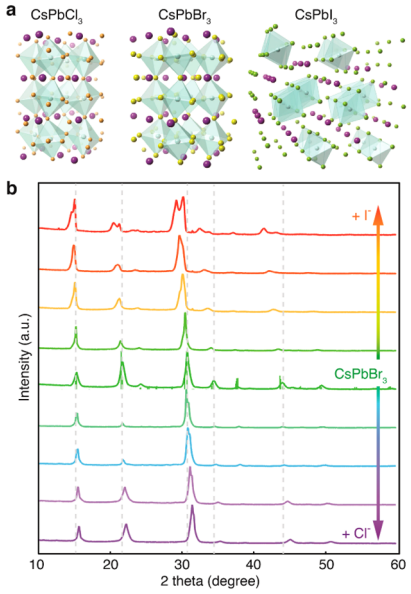

Figure 1. (a) Schematic representations of three $CsPbX_3$ (X = Cl, Br, I) orthorhombic crystal structures. Cs, purple; Pb, blue. (b) XRD patterns of the parent $CsPbBr_3$ NWs and the anion-exchange products, showing the retention of the original corner-sharing orthorhombic phase throughout the exchange reaction. Pattern for orthorhombic $CsPbBr_3$ with ICSD no. 97851 is provided for reference.

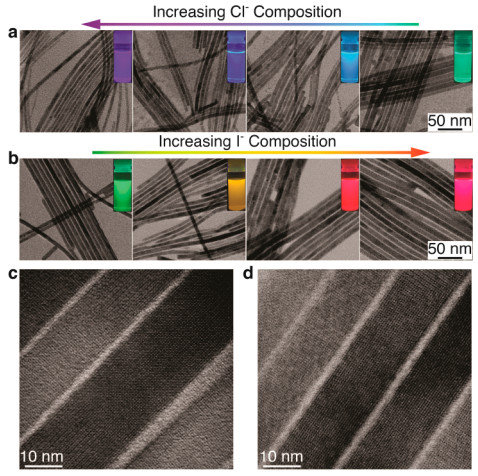

Figure 2. TEM images of $CsPbX_3$ NWs with various degrees of conversion with (a) chloride and (b) iodide anions. The insets show the evolution of emission color (UV excitation, λ = 365 nm) upon forming mixed-halide $CsPb(Br/Cl)_3$ and $CsPb(Br/I)_3$ NWs. HRTEM images of (c) Cl- and (d) I-exchange NWs.

yield (PLQY), time-resolved photoluminescence decay (TRPL), and charge transport measurements demonstrated that anion exchange does not significantly increase the defect density in the NWs.

Colloidal $CsPbBr_3$ NWs with uniform diameters of 10 ± 2 nm were synthesized using our previously reported method with some modifications (Supporting Information (SI)).[10] Notably, by replacing the original oleic acid surfactant with octylamine, the NW yield can be significantly improved, and after simple purification, the purity of the sample can reach about 90% (Figure S1b,c). The XRD pattern for the $CsPbBr_3$ NWs matches well with the standard pattern of the orthorhombic phase (Figures 1b and S1a). However, since the standard pattern of cubic phase mostly overlaps with that of orthorhombic phase (Figure S1a), the possibility of the coexistence of some cubic phase NWs cannot be ruled out. The exchange reactions were carried out under air-free conditions by reacting $CsPbBr_3$ NWs with calculated amounts of I^- or Cl^- precursors (oleylammonium halide (OAmX) or PbX_2) dissolved in oleylamine/oleic acid in octadecene at 80 °C. To improve the NWs' dispersion for the PLQY measurements, surface treatment with the original precursors was performed (SI).

As shown in Figure 1a, pure orthorhombic $CsPbI_3$ has a substantially different crystal structure than orthorhombic $CsPbCl_3$ or $CsPbBr_3$. Orthorhombic $CsPbI_3$ does not have a 3D corner-sharing PbI_6 network but instead contains ribbons of edge-connected PbI_6 octahedra and thus has only quasi-2D connectivity. Nevertheless, we observed that the crystal structure of $CsPbBr_3$ NWs remains corner-sharing orthorhombic after exchange with I^- or Cl^- anions, with only a slight shift in the XRD pattern. This is probably due to the rigidity of the cationic framework that leads to the topotaxial nature of the exchange. The shifts are explained by lattice expansion or contraction caused by the substitution of the larger I^- ion or smaller Cl^- ion, respectively (Figure 1b). We also observed a slight change in XRD peak profile during anion exchange. More specifically, a simulated pattern has been used to fit the experimental XRD pattern of the Br−I alloy, and the calculated lattice parameters show an anisotropic expansion behavior compared to the lattice parameters of the orthorhombic $CsPbBr_3$ (Figure S2), indicating that a slight anisotropic distortion occurred within the lattice during anion exchange. The size and shape of the NWs are also preserved in both the Br−I and Br−Cl exchanges (Figure 2a,b). High-resolution transmission electron microscopy (HRTEM) images of the Br−I and Br−Cl exchange products clearly show the single-crystalline nature of the exchanged NWs, as the absence of epitaxial interfaces and grain boundaries indicates the formation of homogeneous alloy structures (Figures 2c,d and S3). Both cubic and orthorhombic phases have been observed by HRTEM analysis. These cubic phases may occur naturally or are caused by electron beam-induced phase transition, due to the small energy difference between the two phases (no more than $3kT$).[14] The elemental mapping of the exchanged samples was obtained using energy dispersive X-ray spectroscopy (EDS) and also shows a uniform distribution of Cl/I along the whole NWs (Figure S4).

The halide-exchange reactions of $CsPbBr_3$ with different amounts of halide precursors were monitored *ex situ* using absorbance and PL spectroscopy (Figure 3a). The as-grown $CsPbBr_3$ NWs have an emission peak at 519 nm, which gradually red shifts with increased I^- content and reaches a final value of 680 nm. When the I^- precursor was replaced with the Cl^- precursor, the PL peaks of the $CsPbBr_3$ NWs blue shift to shorter wavelengths and eventually reach the shortest wavelength at about 409 nm (Figure 3a, Table S1). The quantitative elemental composition of the alloy is analyzed using EDS (Figure 3b). The band gap calculated from absorption spectra of different alloys was correlated with the elemental composition using a binomial relation (Figure 3b), revealing a significant bowing effect with bowing parameters of −0.55 and 0.67 eV for Br−Cl and Br−I alloys, respectively. Similar bowing is known for other semiconductor alloys, such as zinc chalcogenide or group-III nitride alloys.[16] We observed that, for the most converted Br−I NWs, the I^- percentage is

DOI: 10.1021/jacs.6b03134
J. Am. Chem. Soc. 2016, 138, 7236−7239

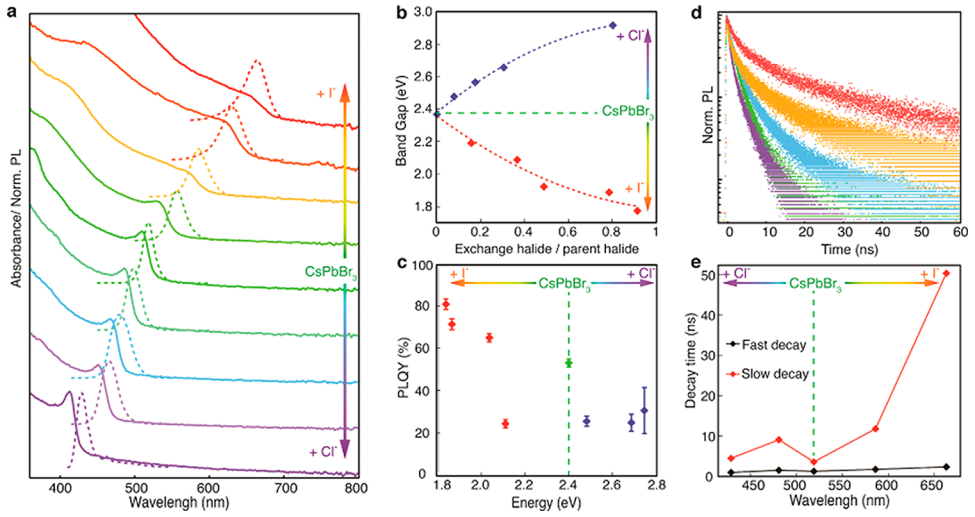

Figure 3. (a) Evolution of the optical absorption (solid lines) and PL (dashed lines) spectra of $CsPbBr_3$ NWs with increasing quantities of exchanged halide sources. (b) Plots of the absorption onset energy (in eV) as a function of iodide content or chloride content. (c) Measured PLQY as a function of the exchanged NWs' bandgap energy. (d, e) TRPL decays and carrier lifetimes of parent $CsPbBr_3$ and anion-exchange products.

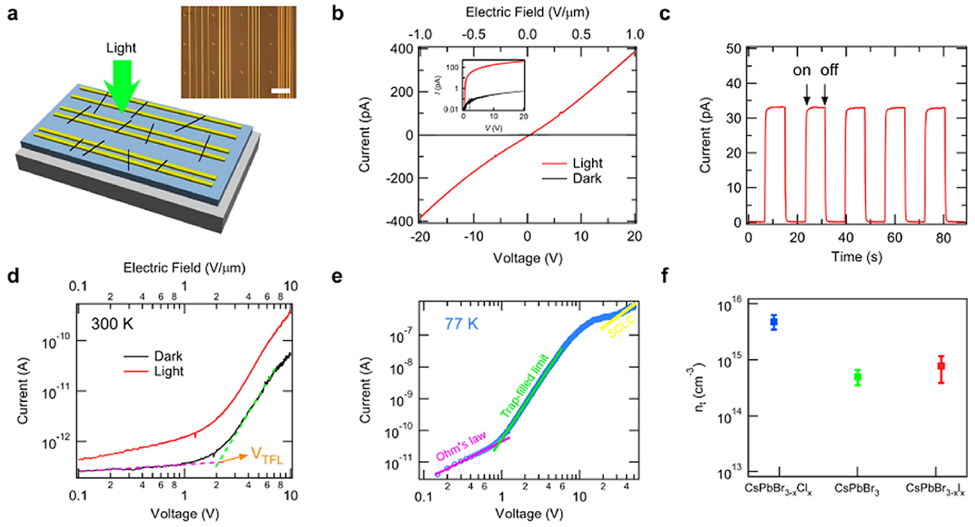

Figure 4. (a) Schematic illustration of the transport measurement setup; the inset shows the optical image of prepatterned gold electrodes for transport measurement (scale bar, 60 μm). (b) $I-V$ characteristics of a typical NW device under dark and light conditions. The light is generated from a solar simulator with an AM 1.5 filter. The device channel width is 20 μm, the inset shows same $I-V$ curve in semilog scale. (c) Photoresponse of the device under a constant bias of 2 V. (d) High electric field $I-V$ curves of another NW device with 1 μm channel width under dark and light conditions. (e) Low-temperature transport measurement of the same device in (d). A fit of the $I-V$ curve is shown for each of the three regimes. (f) Defect density as a function of various compositions. The defect density is calculated based on V_{TFL} at 77K for each composition, $\varepsilon = 4.8$ is used for all samples.[15]

approximately 92%. Increasing the amount of I^- precursor does not further red shift the emission wavelength (Table S1). The distinct crystal structures between orthorhombic $CsPbBr_3$ and $CsPbI_3$ may be the reason for the self-limiting behavior of the Br−I exchange. For the Br−Cl exchanged NWs, quantitative data for the Br−Cl alloy with the largest conversion degree cannot be determined by EDS, due to excess amount of OAmCl which is difficult to clean away. However, the emission wavelength of 8 nm $CsPbCl_3$ nanocubes from direct synthesis (410 nm)[14] suggests the complete substitution of Br^- with Cl^- for the most converted Br−Cl NWs (409 nm). PLQY measurements show overall high QYs for the as prepared (Br, 53 ± 0.7%) and exchanged NWs (I, 81 ± 2.5%, Cl, 30 ± 11%) (Figures 3C and S5). The PLQY increased with the I-exchange reaction, consistent with reports for 0D cubes.[12f] To study the defect-related recombination rate of the $CsPbX_3$ alloy NWs, TRPL decays were measured and fit individually to a biexponential decay function (Figure S6, Table S2). The faster component likely corresponds to surface site recombination and the slower component to bulk recombination. The PL lifetime is in the range of 1−50 ns with longer lifetimes for the iodide-exchanged NWs (Figure 3d,e, Table S2), implying anion exchange does not significantly increase defect-related recombination in these materials.

In order to quantitatively study the defect density level in pure $CsPbBr_3$ and alloy NWs, electrical transport and photocurrent measurements of the NWs were performed. The samples were prepared by drop-casting multiple NW bundles onto prepatterned gold electrodes (Figure 4a). The gaps between the electrodes vary from 1 to 20 μm. Under low

DOI: 10.1021/jacs.6b03134
J. Am. Chem. Soc. 2016, 138, 7236−7239

electric field, a linear $I-V$ characteristic is observed both under dark and light conditions (Figure 4b). The conductance of the NWs increases by 10^3 upon illumination. The photoresponse of the device is fast and free of persistent photocurrent (Figure 4c), indicating a low density of deep trap states which typically exhibit longer response time. We also conducted high electric field measurements on devices with shorter channel widths. As shown in Figure 4d, the dark and photo conductance of the device exhibits a significant nonlinear increase at higher field. The enhanced conductance in shorter channel devices can be attributed to the trap-filled limit (TFL) conduction,[17] where the injected carriers start to fill the defect states in the NW. A more detailed study of the conduction mechanism is performed at 77 K to minimize ion diffusion (Figures 4e and S7). Three regions in the log−log plot of the $I-V$ characteristic are clearly demonstrated. Under low field, the conduction of the NW follows Ohm's law with a linear $I-V$ curve. When the threshold voltage V_{TFL} is reached, the conduction falls into the TFL regime with $I \propto V^n$ ($n > 3$). Further increase of the electric field eventually fills all of the defect states, and we measure a space-charge-limited current for which the conduction is governed by the Mott−Gurney law ($I \propto V^2$).[17] It is worth noticing that these conduction mechanisms can only be resolved in semiconductors with low defect level and poor intrinsic conductivity, such as nearly perfect single crystals.[17] By fitting the $I-V$ curves, one can calculate the defect density as $n_t = 2\varepsilon\varepsilon_0 V_{TFL}/ed^2$, where ε is the dielectric constant,[15] e is the elemental charge, and d is the device channel width. For pure $CsPbBr_3$ NWs, we estimate a defect density of $10^{14}-10^{15}$ cm^{-3}. We note that the defect density may be overestimated, since the ligands on the surface of the NWs can lower the efficiency of charge injection and increase V_{TFL}. The defect density in anion exchanged $CsPbBr_{3-x}Cl_x$ and $CsPbBr_{3-x}I_x$ shows only a slight increase (Figure 4f). The fast photoresponse and high PLQY of the $CsPbX_3$ NWs implies that the existing defects mainly form shallow traps, which is consistent with recent theoretical works that have predicted mainly shallow intrinsic defects in hybrid halide perovskites.[18]

In conclusion, we show that $CsPbBr_3$ NWs with high size monodispersity can be used as templates to independently control the NW composition through anion-exchange reactions. $CsPbX_3$ alloy NWs with a wide range of compositions can be achieved, while retaining the favorable corner-sharing orthorhombic phase. The alloy NWs have bright and tunable PL spanning over nearly the entire visible spectral region, in addition to the favorable optoelectronic properties, making them interesting nanostructures for prospective optoelectronic devices.

■ ASSOCIATED CONTENT

Supporting Information

The Supporting Information is available free of charge on the ACS Publications website at DOI: 10.1021/jacs.6b03134.

Experimental details, additional TEM, EDS, PLQY, TRPL and transport measurement data (PDF)

■ AUTHOR INFORMATION

Corresponding Author

*p_yang@berkeley.edu

Author Contributions

⊥These authors contributed equally to this work.

Notes

The authors declare no competing financial interest.

■ ACKNOWLEDGMENTS

This work was supported by the Director, Office of Science, Office of Basic Energy Sciences, Materials Science and Engineering Division, U.S. Department of Energy under contract no. DE-AC02-05CH11231 (P-Chem). Work at the Molecular Foundry was supported by the office of Science, Office of Basic Energy Sciences of the U.S. Department of Energy under contract no. DE-AC02-05CH11231. D.Z. would like to thank the fellowship support from Suzhou Industrial Park. S.W.E. would like to thank the Camille and Henry Dreyfus Foundation for funding, award no. EP-14-151.

■ REFERENCES

(1) Lu, W.; Lieber, C. M. *Nat. Mater.* **2007**, *6*, 841.
(2) Yan, R.; Gargas, D.; Yang, P. *Nat. Photonics* **2009**, *3*, 569.
(3) Patolsky, F.; Lieber, C. M. *Mater. Today* **2005**, *8*, 20.
(4) Wang, Z. L.; Song, J. *Science* **2006**, *312*, 242.
(5) Morales, A. M.; Lieber, C. M. *Science* **1998**, *279*, 208.
(6) Sun, J.; Buhro, W. E. *Angew. Chem.* **2008**, *120*, 3259.
(7) Han, W.; Fan, S.; Li, Q.; Hu, Y. *Science* **1997**, *277*, 1287.
(8) Cho, K.-S.; Talapin, D. V.; Gaschler, W.; Murray, C. B. *J. Am. Chem. Soc.* **2005**, *127*, 7140.
(9) Lu, X.; Yavuz, M. S.; Tuan, H.-Y.; Korgel, B. A.; Xia, Y. *J. Am. Chem. Soc.* **2008**, *130*, 8900.
(10) Zhang, D.; Eaton, S. W.; Yu, Y.; Dou, L.; Yang, P. *J. Am. Chem. Soc.* **2015**, *137*, 9230.
(11) (a) Stranks, S. D.; Snaith, H. J. *Nat. Nanotechnol.* **2015**, *10*, 391. (b) Zhu, H.; Fu, Y.; Meng, F.; Wu, X.; Gong, Z.; Ding, Q.; Gustafsson, M. V.; Trinh, M. T.; Jin, S.; Zhu, X. Y. *Nat. Mater.* **2015**, *14*, 636.
(12) (a) Li, H.; Zanella, M.; Genovese, A.; Povia, M.; Falqui, A.; Giannini, C.; Manna, L. *Nano Lett.* **2011**, *11*, 4964. (b) Son, D. H.; Hughes, S. M.; Yin, Y.; Paul Alivisatos, A. *Science* **2004**, *306*, 1009. (c) Jain, P. K.; Amirav, L.; Aloni, S.; Alivisatos, A. P. *J. Am. Chem. Soc.* **2010**, *132*, 9997. (d) Wong, A. B.; Lai, M.; Eaton, S. W.; Yu, Y.; Lin, E.; Dou, L.; Fu, A.; Yang, P. *Nano Lett.* **2015**, *15*, 5519. (e) Nedelcu, G.; Protesescu, L.; Yakunin, S.; Bodnarchuk, M. I.; Grotevent, M. J.; Kovalenko, M. V. *Nano Lett.* **2015**, *15*, 5635. (f) Akkerman, Q. A.; D'Innocenzo, V.; Accornero, S.; Scarpellini, A.; Petrozza, A.; Prato, M.; Manna, L. *J. Am. Chem. Soc.* **2015**, *137*, 10276. (g) Bekenstein, Y.; Koscher, B. A.; Eaton, S. W.; Yang, P.; Alivisatos, A. P. *J. Am. Chem. Soc.* **2015**, *137*, 16008. (h) Akkerman, Q. A.; Motti, S. G.; Srimath Kandada, A. R.; Mosconi, E.; D'Innocenzo, V.; Bertoni, G.; Marras, S.; Kamino, B. A.; Miranda, L.; De Angelis, F.; Petrozza, A.; Prato, M.; Manna, L. *J. Am. Chem. Soc.* **2016**, *138*, 1010.
(13) (a) Mizusaki, J.; Arai, K.; Fueki, K. *Solid State Ionics* **1983**, *11*, 203. (b) Eames, C.; Frost, J. M.; Barnes, P. R.; O'Regan, B. C.; Walsh, A.; Islam, M. S. *Nat. Commun.* **2015**, *6*, 7497.
(14) Protesescu, L.; Yakunin, S.; Bodnarchuk, M. I.; Krieg, F.; Caputo, R.; Hendon, C. H.; Yang, R. X.; Walsh, A.; Kovalenko, M. V. *Nano Lett.* **2015**, *15*, 3692.
(15) Eaton, S. W.; Lai, M.; Gibson, N. A.; Wong, A. B.; Dou, L.; Ma, J.; Wang, L. W.; Leone, S. R.; Yang, P. *Proc. Natl. Acad. Sci. U. S. A.* **2016**, *113*, 1993.
(16) Bernard, J. E.; Zunger, A. *Phys. Rev. B: Condens. Matter Mater. Phys.* **1986**, *34*, 5992.
(17) (a) Shi, D.; Adinolfi, V.; Comin, R.; Yuan, M.; Alarousu, E.; Buin, A.; Chen, Y.; Hoogland, S.; Rothenberger, A.; Katsiev, K.; Losovyj, Y.; Zhang, X.; Dowben, P. A.; Mohammed, O. F.; Sargent, E. H.; Bakr, O. M. *Science* **2015**, *347*, 519. (b) Lampert, M. A.; Mark, P. *Current injection in solids*; Academic Press: New York, 1970.
(18) Kim, J.; Lee, S. H.; Lee, J. H.; Hong, K. H. *J. Phys. Chem. Lett.* **2014**, *5*, 1312.

DOI: 10.1021/jacs.6b03134
J. Am. Chem. Soc. 2016, 138, 7236−7239